

Supporting Information

**Precise Formation of a Hollow Carbon Nitride Structure with a Janus Surface to Promote Water Splitting by Photoredox Catalysis**

*Dandan Zheng, Xu-Ning Cao, and Xinchun Wang\**

anie\_201606102\_sm\_miscellaneous\_information.pdf

## Supporting Information

### Experimental Section

**Synthesis of  $m\text{SiO}_2/\text{Pt}/\text{SiO}_2$  nanospheres template:** First, the monodisperse  $\text{SiO}_2$  template were synthesized according to the Stöber method. Briefly, 3.10 g of aqueous ammonia (32 wt.%, Sigma-Aldrich) and 10 g of deionized water were added in 58.5 g of ethanol to form a mixture solution after stirring for 30 min at 30 °C. 5.6 ml of tetraethoxysilane (TEOS, Sigma-Aldrich) was added to the above solution with vigorous stirring and was left stationary for 1 h to yield uniform nonporous silica spheres. After washing twice with ethanol by centrifugation and redispersion, the particles were transferred to a mixture of isopropanol (50 g) and 3 g 3-Aminopropyl-triethoxysilane (APTES, Sigma-Aldrich) and heated to 80 °C for 2 hours to functionalize the silica surface with  $-\text{NH}_2$  groups. The surface modified particles were washed with ethanol and dispersed in a mixture solution with ethanol (58.5g), deionized water (10 g) and 3.10 g of aqueous ammonia. A mixture of adequate TEOS and *n*-octadecyltrimethoxysilane (C18-TMOS, Sigma-Aldrich) was then added dropwise to the above solution with magnetic stirring, sat quietly maturing for another 3 h at ambient temperature. The nanostructured silica was centrifuged, dried at 70 °C and calcined at 550 °C for 6 h in air.

**Synthesis of HCNS/Pt:** The as-prepared  $m\text{SiO}_2/\text{Pt}/\text{SiO}_2$  templates were neutralized with a 1-M HCl solution and then dried at 80 °C overnight. Then, these monodisperse silica nanoparticles were used as a template to prepare HCNS. 2 g of the  $\text{SiO}_2$  template was added to 10 g of cyanamide (Alfa Aesar), and kept under sonication and vacuum at 60 °C for 2 h. After that, the mixture was stirred at 60 °C overnight, which was then centrifuged, dried, and calcined at 550 °C for 4 h. The obtained powder was treated with 4 M  $\text{NH}_4\text{HF}_2$  for 12 h to remove the silica template, then centrifuged and washed three times with distilled water and once with ethanol. The final yellow HCNS powders were obtained by drying at 80 °C in a vacuum oven overnight.

**Synthesis of  $\text{Co}_3\text{O}_4/\text{HCNS}/\text{Pt}$ :** The monodispersed  $\text{Co}_3\text{O}_4$  NPs was synthesized according to the literature. The prepared  $\text{Co}_3\text{O}_4$  NPs were dispersed in methanol with the desired concentration ( $0.5\text{mg}\cdot\text{mL}^{-1}$ ), which was then subject to ultrasonic treatment for 30 min to promote the dispersion of  $\text{Co}_3\text{O}_4$  in the solution. HCNS/Pt samples powder was first dispersed in 5mL methanol, and then a certain amount of the  $\text{Co}_3\text{O}_4$  solution was added to the mixture. After drying in oil bath, the mixture was transferred to a vacuum oven and kept at 60°C overnight to remove the methanol. To strengthen the interaction between  $\text{Co}_3\text{O}_4$  NPs and the carbon nitride matrix, the resulting mixture was further treated at 150°C for 2h in air. The obtained samples were denoted as  $X\%\text{Co}_3\text{O}_4/\text{HCNS}/M\%\text{Pt}$ , where X and M refers to the weight percentages of  $\text{Co}_3\text{O}_4$  and Pt, respectively, according to HCNS weight.

**Synthesis of  $(\text{Co}_3\text{O}_4 + \text{Pt})/\text{HCNS}$ :** The prepared Pt and  $\text{Co}_3\text{O}_4$  NPs with suitable amount were loading on the out surface of HCNS, same method with synthesis of  $\text{Co}_3\text{O}_4/\text{HCNS}/\text{Pt}$  sample.

**Characterization:** The morphology of the sample was investigated by field emission scanning electron microscopy (SEM) (JSM-6700F). Transmission electron microscopy (TEM) was obtained by Zeis 912 microscope. The nitrogen adsorption–desorption isotherms were collected at 77 K using Micromeritics ASAP 2020 Surface Area and Porosity Analyzer. Powder X-ray diffraction (XRD) measurements were performed on Bruker D8 Advance diffractometer with Cu K $\alpha$ 1 radiation ( $k = 1.5406 \text{ \AA}$ ). Fourier transformed infrared (FTIR) spectra were recorded on BioRad FTS 6000 spectrometer. X-ray photoelectron spectroscopy (XPS) data were obtained on Thermo ESCALAB250 instrument with a monochromatized Al K $\alpha$  line source (200 W). UV–Vis diffuse reflectance spectra (UV–Vis DRS) were performed on Varian Cary 500 Scan UV–visible system. Photoluminescence spectra were recorded on an Edinburgh F1/FSTCSPC 920 spectrophotometer. Electrochemical measurements were conducted with a BAS Epsilon Electrochemical System in a conventional three electrode cell, using a Pt plate as the counter electrode and an Ag/AgCl electrode (3 M KCl) as the reference electrode. The working electrode was prepared on indium-tin oxide (ITO) glass that was cleaned by sonication in ethanol for 30 min and dried at 353 K. The boundary of ITO glass was protected using Scotch tape. The 5 mg sample was dispersed in 1 mL of DMF by sonication to get a slurry. The slurry was spread onto pretreated ITO glass. After air-drying, the working electrode was further dried at 393 K for 2 h to improve adhesion. Then, the Scotch tape was unstuck, and the uncoated part of the electrode was isolated with epoxy resin.

**Activity Testing:** Photocatalytic H<sub>2</sub> production was carried out in a Pyrex top-irradiation reaction vessel connected to a glass-closed gas circulation system. For each reaction, 20 mg well-ground catalyst powder was dispersed in an aqueous solution (100 mL) containing triethanolamine (10 vol.%) as sacrificial electron donor. The reactant solution was evacuated several times to remove air completely prior to irradiation under a 300W Xe lamp and a water-cooling filter. The wavelength of the incident light was controlled by using an appropriate long pass cut-off filter. The temperature of the reactant solution was maintained at room temperature by a flow of cooling water during the reaction. The evolved gases were analyzed by gas chromatography equipped with a thermal conductive detector (TCD) with argon as the carrier gas.

Photocatalytic O<sub>2</sub> production was measured in a Pyrex top-irradiation reaction vessel connected to a glass closed gas circulation system. For each reaction, 20 mg catalyst powder was well dispersed in an aqueous solution (100 mL) containing AgNO<sub>3</sub> (0.01M) as an electron acceptor and La<sub>2</sub>O<sub>3</sub> (0.2g) as a pH buffer agent. The reactant solution was evacuated several times to remove air completely prior to irradiation under a 300 W Xe lamp and a water-cooling filter. The wavelength of the incident light was controlled by using an appropriate long pass cut-off filter. The temperature of the reactant solution was maintained at room temperature by a flow of cooling water during the reaction. The evolved gases were analyzed by gas chromatography equipped with a thermal conductive detector (TCD) with argon as the carrier gas.

Overall water splitting was carried out in a Pyrex top-irradiation reaction vessel connected to a glass closed gas circulation system. For each reaction, 20 mg catalyst powder was well dispersed in an aqueous solution (100 mL). The reactant solution was evacuated several times to remove air completely prior to irradiation under a 300 W Xe lamp and a water-cooling filter. The wavelength of the incident light was

---

controlled by using an appropriate long pass cut-off filter. The temperature of the reactant solution was maintained at room temperature by a flow of cooling water during the reaction. The evolved gases were analyzed by gas chromatography equipped with a thermal conductive detector (TCD) with argon as the carrier gas.

WILEY-VCH

---

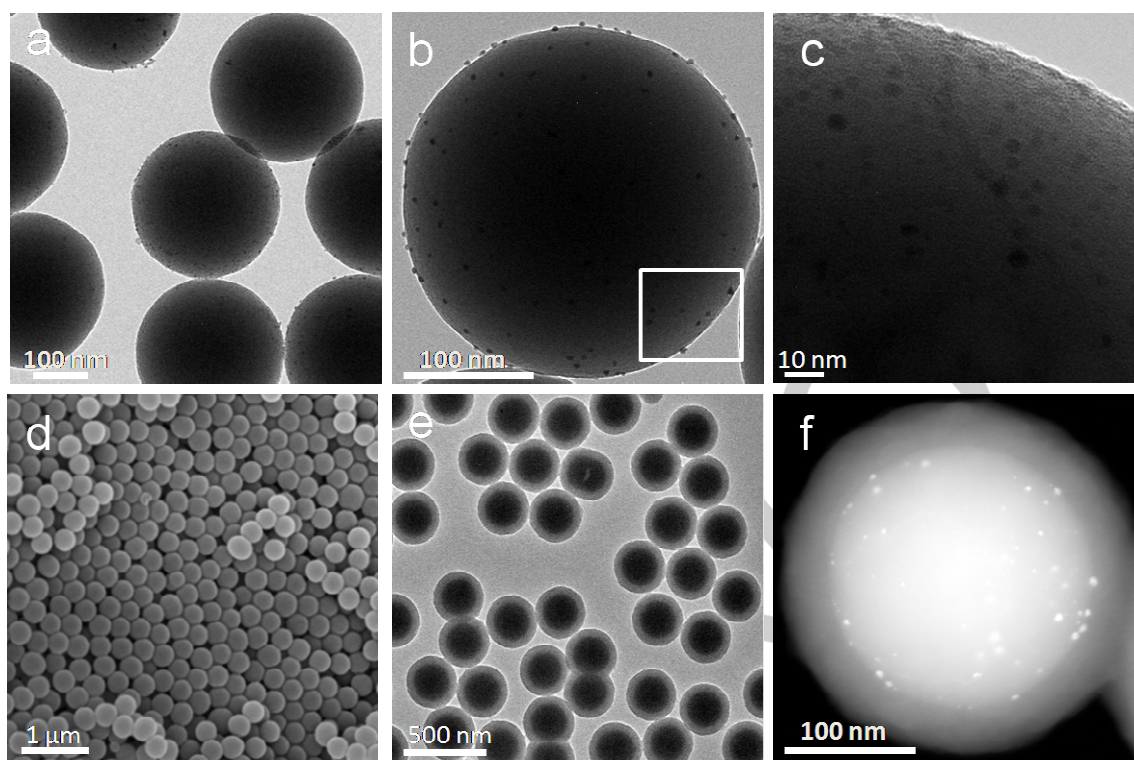


**Figure S1.** (a, b) TEM, and (c) HRTEM images of Pt/SiO<sub>2</sub> template. (d) SEM and (e, f) TEM images of mSiO<sub>2</sub>/Pt/SiO<sub>2</sub> templates.

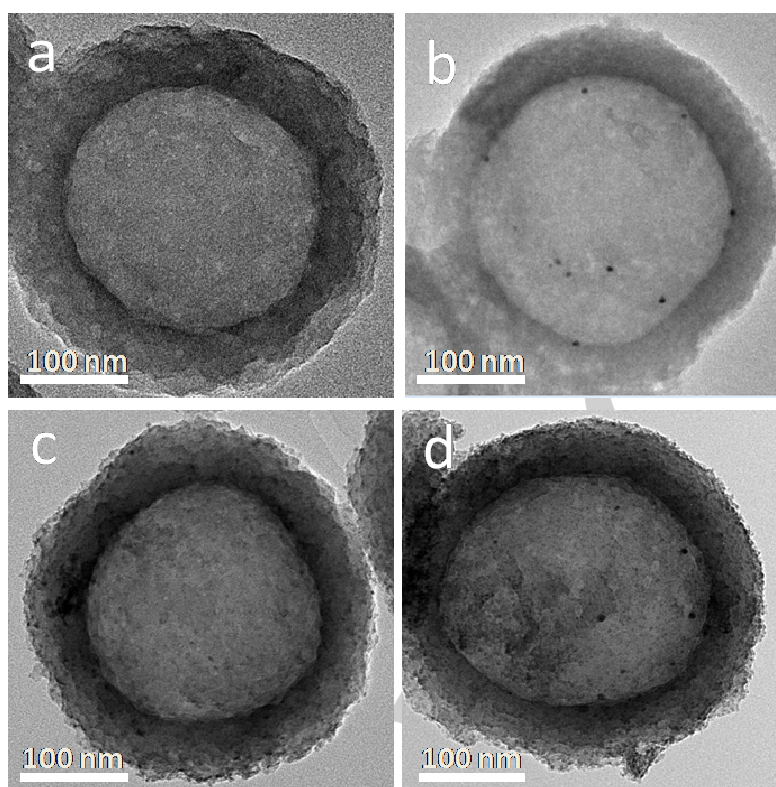


**Figure S2.** TEM images of (a) HCNS, (b) HCNS/Pt, (c)  $\text{Co}_3\text{O}_4/\text{HCNS}$ , (d)  $\text{Co}_3\text{O}_4/\text{HCNS}/\text{Pt}$  samples.

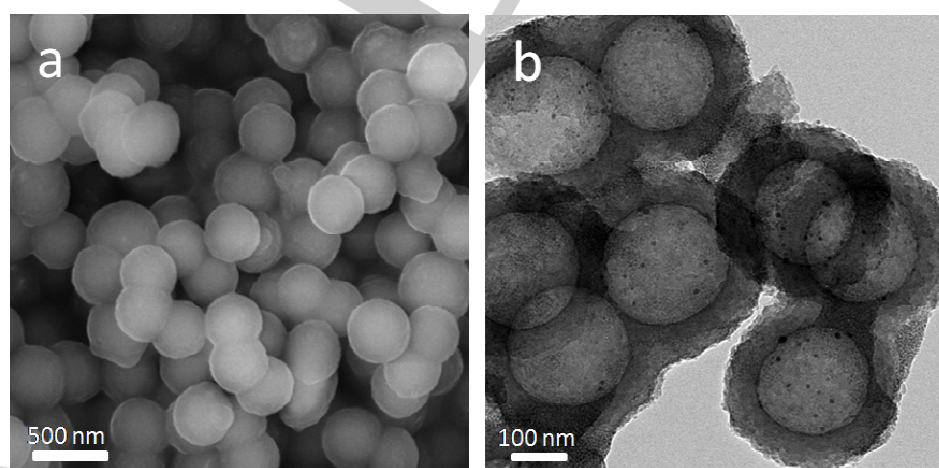


**Figure S3.** (a) SEM and (b) TEM images of  $\text{Co}_3\text{O}_4/\text{HCNS}/\text{Pt}$  samples.

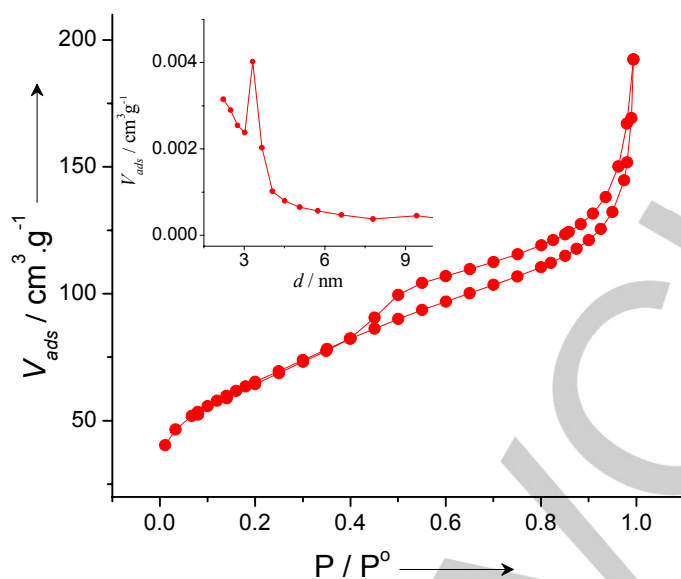


**Figure S4.** N<sub>2</sub> adsorption-desorption isotherms and the corresponding Barrett-Joyner-Halenda pore-size distribution (inset) of Co<sub>3</sub>O<sub>4</sub>/HCNS/Pt samples.

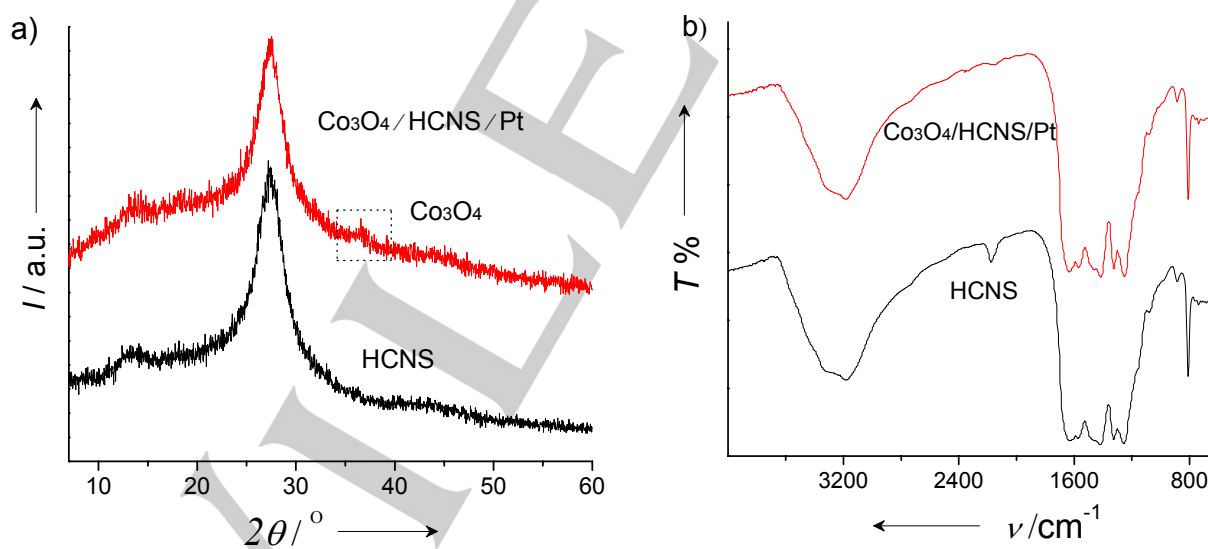


**Figure S5.** Physical characterizations of Co<sub>3</sub>O<sub>4</sub>/HCNS/Pt, together with HCNS as a reference. (a) XRD patterns, (b) FT-IR spectra. No characteristic peaks of crystallized Pt NPs can be found in the XRD patterns because of the loading amount of Pt NPs is very low (only 2wt.%).

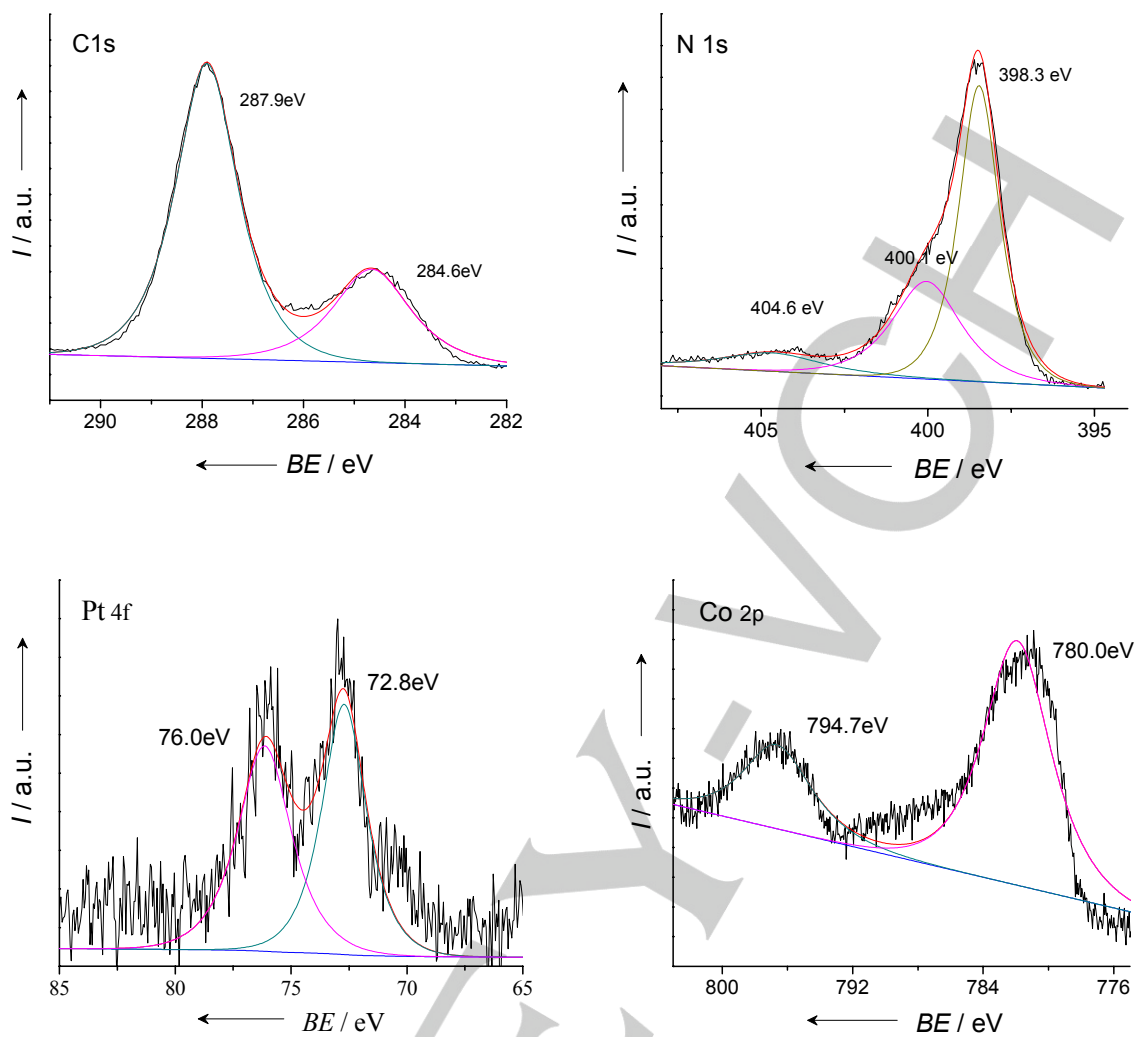


Figure S6. XPS analysis of  $\text{Co}_3\text{O}_4/\text{HCNS}/\text{Pt}$  samples.

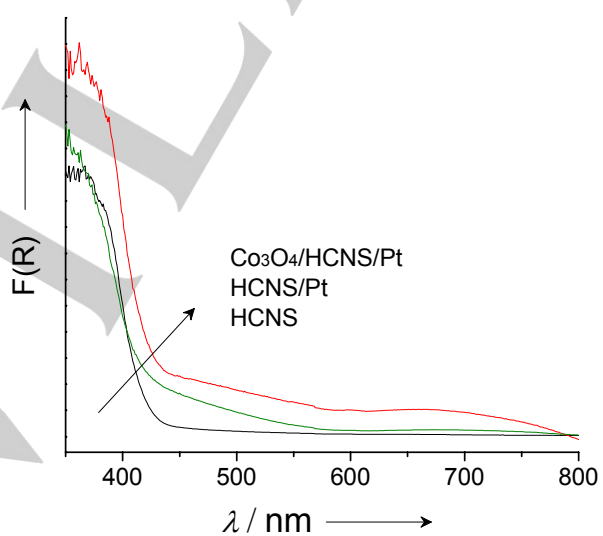
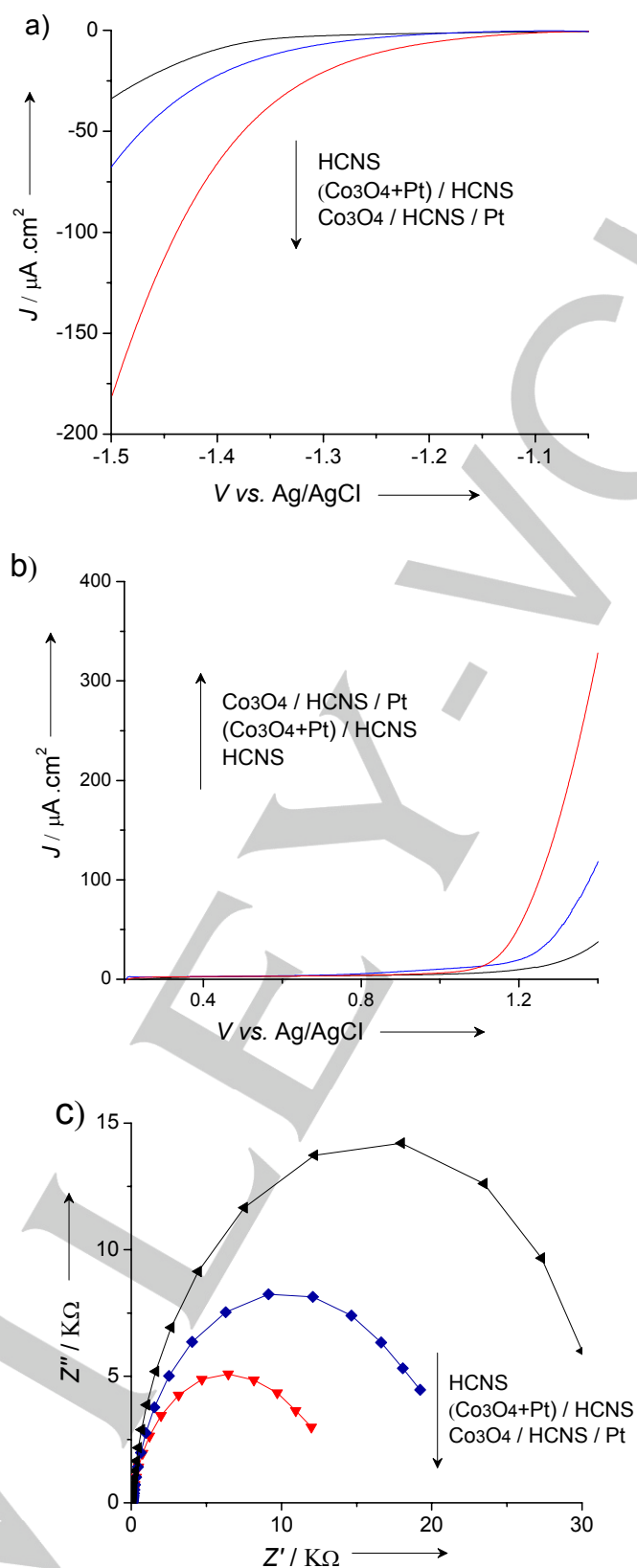
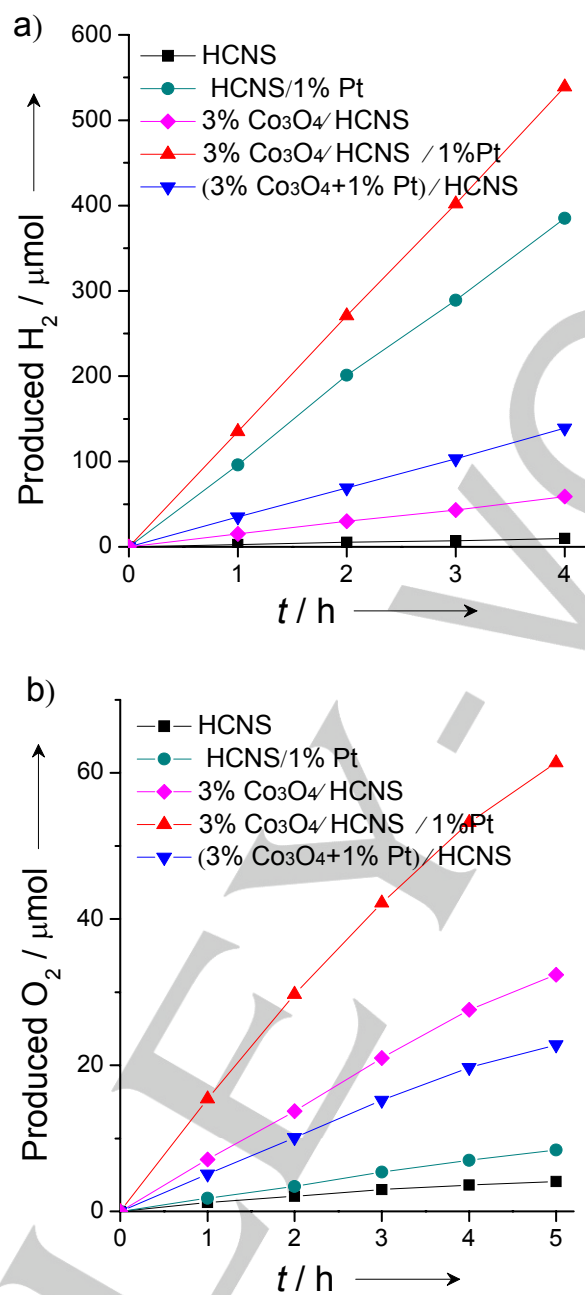


Figure S7. UV-Vis diffuse reflectance spectra of  $\text{Co}_3\text{O}_4/\text{HCNS}/\text{Pt}$ ,  $\text{HCNS}/\text{Pt}$  and  $\text{HCNS}$  samples.





**Figure S8.** a) b) Polarization curves and c) EIS Nyquist plots of Co<sub>3</sub>O<sub>4</sub>/HCNS/Pt electrode, together with HCNS and (Co<sub>3</sub>O<sub>4</sub>+Pt)/HCNS as reference.



**Figure S9.** a) H<sub>2</sub> evolution activities under visible light irradiation and b) O<sub>2</sub> evolution activities under UV irradiation ( $\lambda > 300$  nm) of HCNS photocatalysts with separated and mixed Pt and Co<sub>3</sub>O<sub>4</sub> cocatalysts.

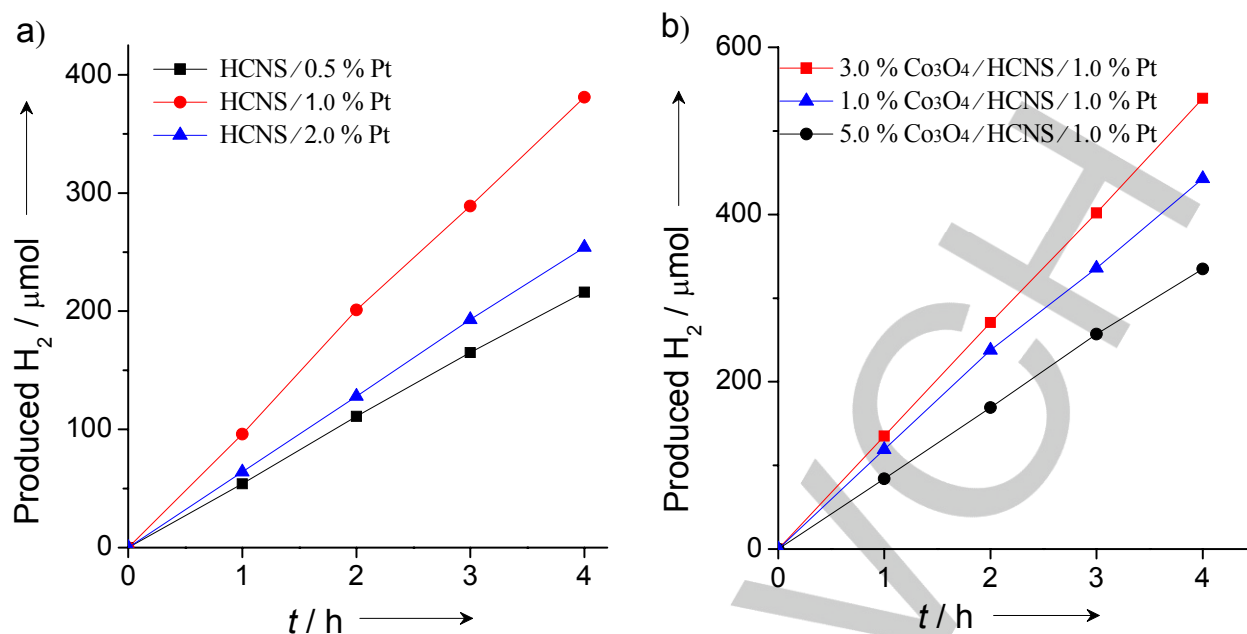


**Figure S10.** (a) Pt NPs loading amount dependence of the rate of H<sub>2</sub> evolution over HCNS photocatalysts under visible light irradiation ( $\lambda > 420$  nm). (b) Time courses of H<sub>2</sub> evolution on HCNS/Pt photocatalysts with different loading amount of Co<sub>3</sub>O<sub>4</sub> under visible light irradiation ( $\lambda > 420$  nm).

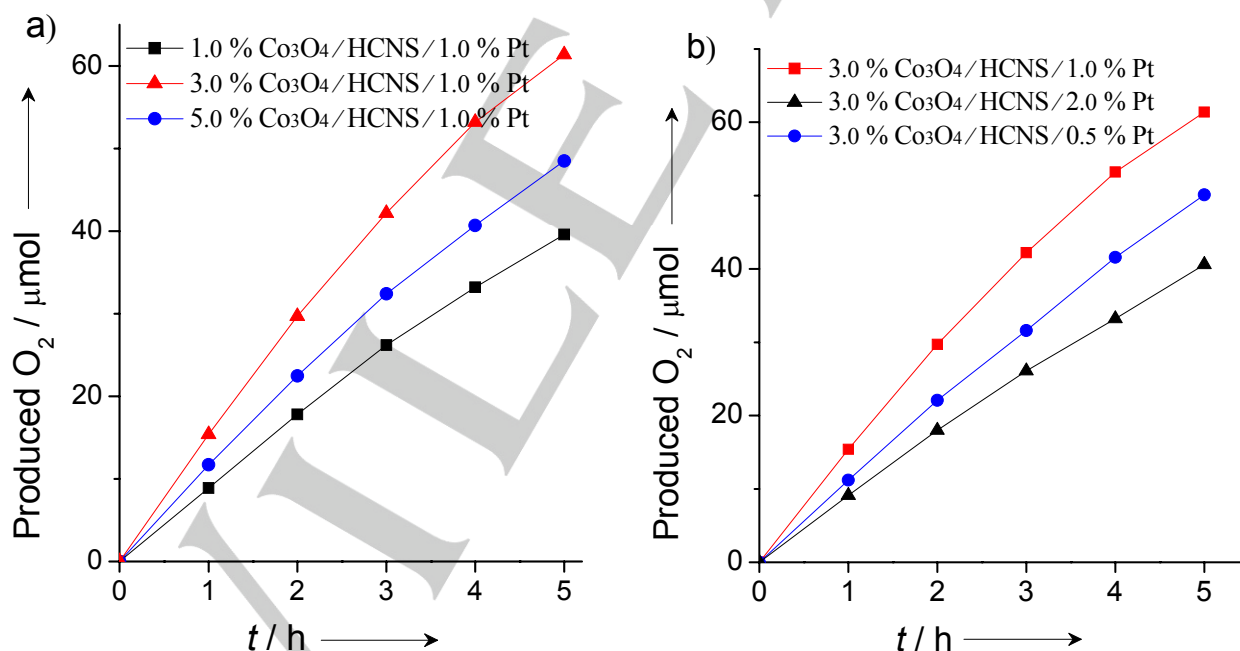


**Figure S11.** Pt and Co<sub>3</sub>O<sub>4</sub> loading amount dependence of the rate of O<sub>2</sub> evolution over HCNS photocatalysts with separated cocatalysts under UV irradiation ( $\lambda > 300$  nm). The loading amounts of Pt were changed at the loading of 3 wt% Co<sub>3</sub>O<sub>4</sub>, while those of Co<sub>3</sub>O<sub>4</sub> were changed at the loading of 1 wt% Pt.

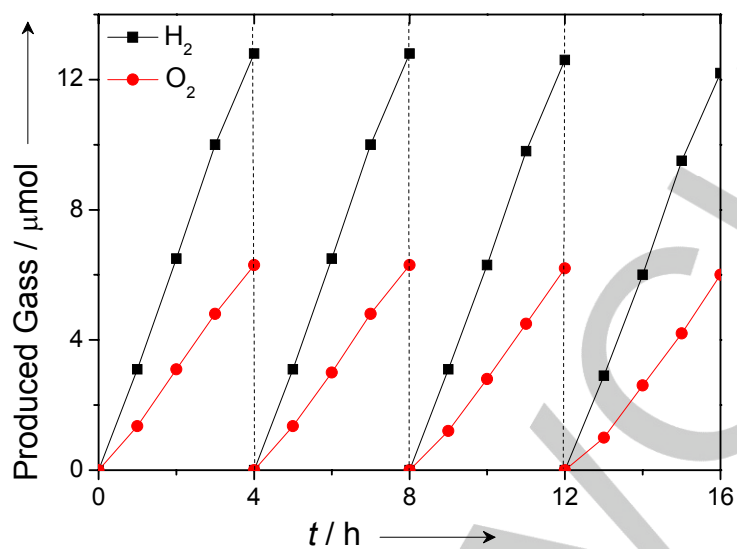


**Figure S12.** The stability test of  $\text{Co}_3\text{O}_4/\text{HCNS}/\text{Pt}$  photocatalysts for overall water splitting under UV irradiation ( $\lambda > 300$  nm).

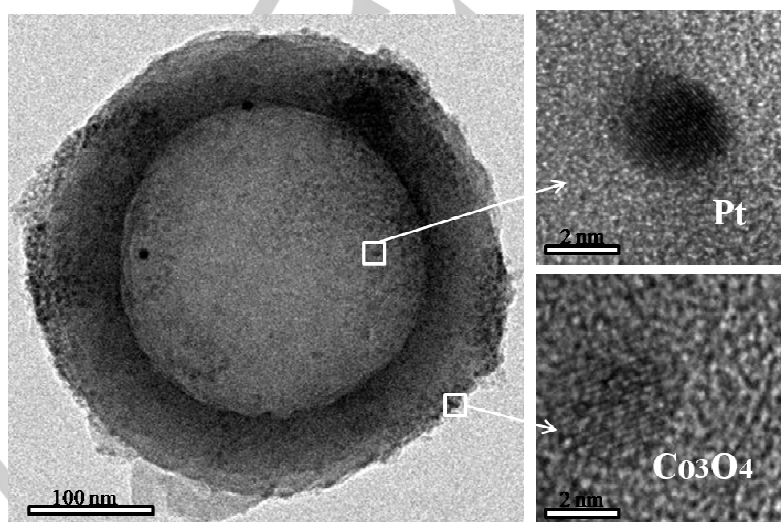


**Figure S13.** TEM images of the  $\text{Co}_3\text{O}_4/\text{HCNS}/\text{Pt}$  sample recovered after the photocatalytic reaction.

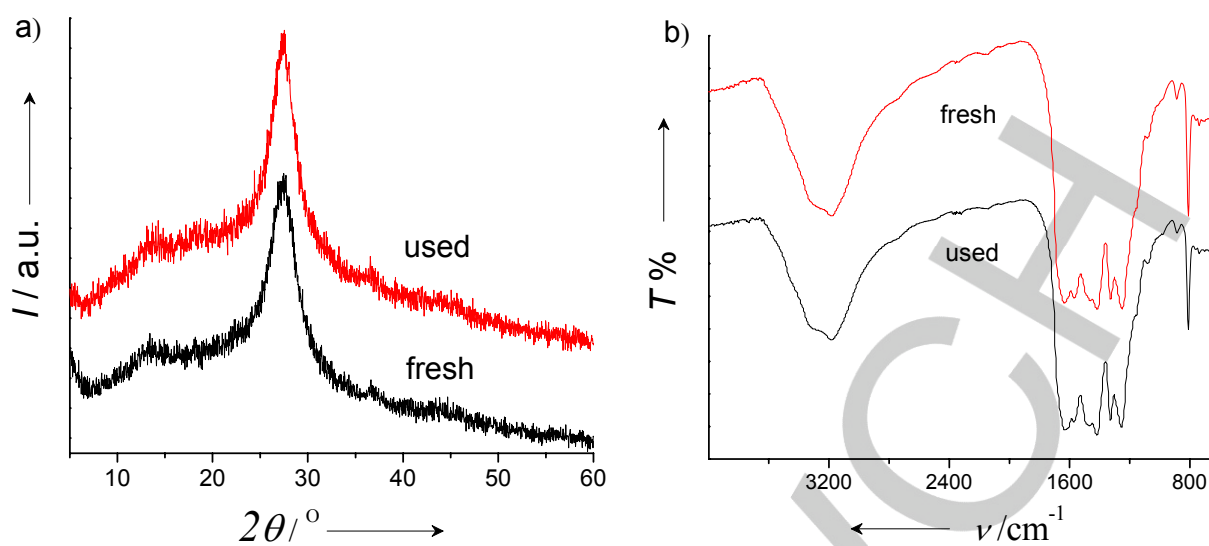


**Figure S14.** Structure of  $\text{Co}_3\text{O}_4/\text{HCNS}/\text{Pt}$  before and after the photochemical reaction. a) XRD pattern, b) FTIR spectra.